Rapid sacrificial layer etching for the fabrication of nanochannels with integrated metal electrodes

Wouter Sparreboom, Jan C. T. Eijkel, Johan Bomer and Albert van den Berg*

Received 24th October 2007, Accepted 14th December 2007
First published as an Advance Article on the web 15th January 2008
DOI: 10.1039/b716382g

We present a rapid etch method to surface-micromachine nanochannels with integrated noble metal electrodes using a single metal sacrificial layer. The method is based on the galvanic coupling of a chromium sacrificial layer with gold electrodes, which results in a 10-fold increase in etch rate with respect to conventional single metal etching. The etch process is investigated and characterized by optical and electrochemical measurements, leading to a theoretical explanation of the observed etch rate based on mass transport. Using this explanation we derive some generic design rules for nanochannel fabrication employing sacrificial metal etching.

1 Introduction

Nanofluidic systems have an inherent large surface to volume ratio. This renders them interesting for integration with sensor and actuator systems, *e.g.* to manipulate and sense large biomolecules such as DNA.[1] However, most nanofluidic systems reported in the literature are fabricated by bulk micromachining,[2–5] which complicates the integration into more complex systems.[6,7] In bulk-micromachining nanochannels are created by etching trenches and/or cavities in one wafer and bonding a second one on top of the first. An alternative to this fabrication method is surface-micromachining,[6–11] where all structures are created on the surface of a single wafer and no bonding step is needed. In surface-micromachining a nanochannel is often created using a sacrificial layer which is covered by a thin film (capping layer). Different sacrificial materials have been proposed in the literature.[6,9,10] However, most of them need to be etched away from one or both side-ends of the channel, which is a slow process (from days up to weeks depending on the length of the channels), because it is limited by the transport of etchant and waste products, usually by diffusion. Several solutions for this problem are given in the literature,[11–13] such as employing a sacrificial polymer that evaporates through the capping layer upon heating.[12,13] However, most of them require either special materials or geometries of the capping layer, which does not make them especially useful to create complex systems with for example integrated electrodes. Recently, a novel method was proposed[14] in which two dissimilar galvanically coupled metals are used as a sacrificial layer. The etch rate of this method is up to 10 times higher than in conventional methods.

In this paper we show that this method is eminently suitable to fabricate nanochannels with integrated bare electrodes using a single sacrificial metal layer. The method is based on the galvanic coupling of a sacrificial chromium layer with gold electrodes. In Fig. 1 a micrograph and a schematic front view of the device are given. In the future we plan to use this device to electrostatically manipulate ions and charged molecules in a nanochannel with double layer overlap as proposed in ref. 6. The electrodes can be actuated using traveling waves, as is done in microchannels by ref. 15 and 16. An additional application would be electrochemical and/or electric impedance sensing inside the channel. Furthermore, we provide a theoretical explanation of the enhanced etch rate based on mass transport considerations and we investigate the kinetics by performing polarization measurements. A thorough understanding of the underlying processes is important for the design of future devices. Finally,

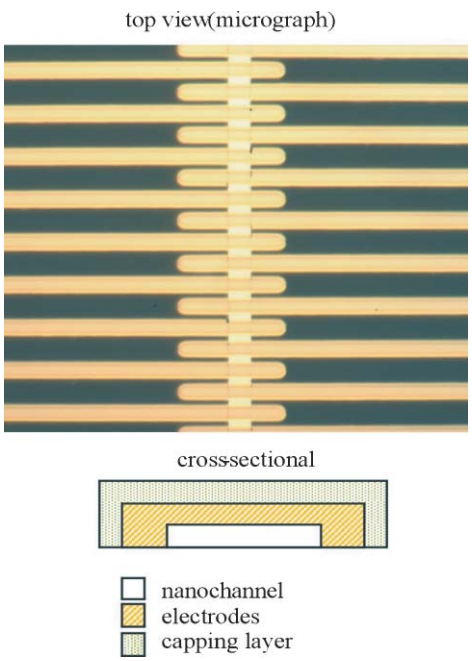

Fig. 1 Micrograph and schematic drawing of the device prior to etching at 63× magnification. In this picture the nanochannel runs from top to bottom and the electrodes from left to right.

BIOS, the Lab-on-a-chip Group, MESA+ Institute for Nanotechnology, University of Twente, PO Box 217, 7500, AE, Enschede, The Netherlands. E-mail: a.vandenberg@ewi.utwente.nl; Fax: +31 534892287; Tel: +31 534892691

we offer some generic design rules for nanochannel fabrication employing sacrificial metal etching.

2 Theory

In this study we remove the sacrificial layer by a wet etchant and enhance the etch rate by galvanic coupling to gold. The etchant has two functions. First, electrochemically oxidize the metal by an electrochemical couple that is higher in the electrochemical series than the metal. Second, dissolve the generated metal ions. In this study the sacrificial metal is chromium and the etchant contains cerium(IV). In eqn (1) the electrochemical reactions are given.

$$\begin{aligned} &Cr(s) \Leftrightarrow Cr^{3+}(aq) + 3e^- \\ &Cr(s) + 3Ce^{4+}(aq) \Leftrightarrow Cr^{3+}(aq) + 3Ce^{3+}(aq) \\ &3Ce^{4+}(aq) + 3e^- \Leftrightarrow 3Ce^{3+}(aq) \end{aligned} \quad (1)$$

Because cerium(IV) is higher in the electrochemical series than chromium the reaction above will go from left to right and the chromium is etched. The higher the difference in standard potential between the metal and the etchant the higher the etch rate in a bulky etchant. There are two ways of obtaining an additional increase in etch rate of a metal: (1) galvanic coupling to a metal with a higher standard potential; (2) applying an external electric potential to the metal that is positive with respect to the etchant. The first case can only be applied in combination with an etchant, the second can be applied without, however the metal should be in contact with an electrolyte that is able to dissolve the generated metal ions. In this paper we test 1 and a combination of 1 and 2.

We assume that etching in our system is a steady state process and that the Nernst equation applies, therefore, we can describe the electric potential of chromium by eqn (2).

$$E = E_{0,Cr} + \frac{RT}{z_+F} \ln\left(\frac{Cr^{3+}(aq)}{Cr(s)}\right) \quad (2)$$

Here, $E_{0,Cr}$ [V] is the standard electrode potential of chromium; F [C mol^{-1}] and R [J K^{-1} mol^{-1}] represent the Faraday and the universal gas constant, respectively; z_+ is the valence; T [K] is the temperature and $Cr^{3+}(aq)$ [mol m^{-3}] and Cr(s) [mol m^{-3}] represent the concentration of chromium ions and solid chromium, respectively. In electrochemistry Cr(s) is usually taken as unity.[17] Eqn (2) shows that as the concentration of chromium ions increases, the potential of the chromium increases. The consequence of this is that the potential difference between the chromium and etchant is effectively decreased for increasing chromium ion concentrations at the metal interface, thereby, decreasing the etch rate. In our system reagents and products have to be transported through a 1-D channel, therefore, mass transport is probably a limiting factor as in most systems where convection is negligible.[17] This means that as the potential difference increases, the concentration of chromium ions at the metal surface increases which counteracts the increase in potential difference. Therefore, there will be a steady state etch rate based on the trade-off between potential difference and mass transport limitations. In the following subsection two etching mechanisms based on mass transport are proposed.

Proposed etching mechanisms

We derived two concepts for etching, one for a single metal sacrificial layer and one for galvanically coupled metals where the chromium forms the sacrificial layer (see Fig. 2). In the first case, the etching of the chromium and the reduction of the etchant both occur at the etch front. Therefore, transport is limited by the diffusion of reagents to and reaction products from the etch front. In the second case, the oxidation of the metal occurs at the etch front in the nanochannel, whilst the reduction of the etchant occurs both at the etch front and outside the channel at the gold surface. Since, the gold surface is much larger and more easily accessible, the reduction will occur mainly at the gold surface outside the channel. In this

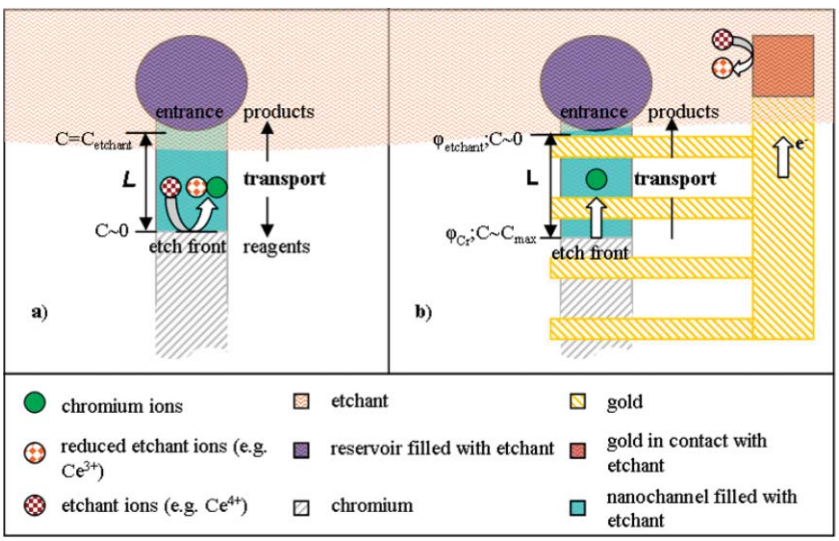

Fig. 2 Proposed etching mechanisms: (a) Single metal sacrificial layer, transport is diffusion driven. The driving concentration difference is ~0.2 M. (b) Galvanically coupled sacrificial layer, transport diffusion and migration driven. The driving concentration difference can be up to 5 M, depending on the metal and the etchant.

case, chromium transport is driven not only by diffusion, but also by migration of reaction products from the etch front due to the potential difference between the metal and the electrolyte. Furthermore, the diffusional transport in the second case can be much higher, because it is only limited by the maximum solubility of chromium and not by the etchant concentration as in the first case. The magnitude of the concentration difference that drives the diffusional transport is dependent on the energy level and hence the electric potential of the metal couple with respect to the etchant.

Mass transport is assessed by the Nernst–Planck equations.[18] These equations describe the current density as a function of diffusion, migration and convection. In our analysis we neglect convection and only consider diffusion and migration. Because of the 1-D geometry of the channel, we will only consider longitudinal mass transport. For clarity, the simplified equations are given below.

$$i_+ = -D_+ F z_+ \frac{\partial c_+}{\partial x} - \frac{F^2 z_+^2 D_+ c_+}{RT}\frac{\partial \varphi}{\partial x} \tag{3a}$$

$$i_- = -D_- F z_- \frac{\partial c_-}{\partial x} - \frac{F^2 z_-^2 D_- c_-}{RT}\frac{\partial \varphi}{\partial x} \tag{3b}$$

Here, $i_\pm$ [A m^{-2}] describe the current density caused by cation and anion transport, respectively; $D_\pm$ [m^2 s^{-1}], $z_\pm$ and $C_\pm$ [mol m^{-3}] represent the diffusion constants, the valence (*i.e.* positive for cations and negative for anions) and the concentration of the ions in the system, respectively; ϕ [V] represents the electric potential and x [m] is the position and is defined in the axial direction. To avoid creating a (complicated) moving boundary problem, we assume that the movement of the etch front does not affect the amount of chromium ions per unit time generated at the etch front and removed from it, which results in the assumption that the concentration of chromium ions at the etch front is constant in time. Furthermore, we assume that the electric current in the system with the etch front at a specific position is constant. To translate current density to the length, L [m], which has been etched, we derived the following equation.

$$L = \sqrt{2\int_0^L \int_0^t \frac{MW}{\rho}\frac{i_+}{zF}\mathrm{d}t\mathrm{d}x} \tag{4}$$

Here MW [kg m^{-3}] and ρ [kg mol] are the molecular weight and the density of chromium, respectively and t [s] is the elapsed time. To derive an equation that describes L as a function of the concentration at the etch front, we solved eqn (3a) for c_+. For this derivation we used a comparable method to ref. 18. With the assumptions made above, in this case, the migration of anions towards the etch front is counterbalanced by their diffusion away from the etch front. This results in a zero net current of anions, so we can express the potential gradient as a concentration gradient by solving eqn (3b) for $i_- = 0$.

$$\frac{\partial \varphi}{\partial x} = -\frac{RT}{Fz_- c}\frac{\partial c}{\partial x} \tag{5}$$

We substitute the result in eqn (3a). After substitution, we integrate eqn (3a) with respect to x and rearrange terms to obtain the concentration of chromium ions as a function of position, $c(x)$. As a boundary condition at the channel entrance we use $c = c_\mathrm{b}$, where c_b [mol m^{-3}] is the bulk concentration of chromium ions. The result is given in eqn (6).

$$c(x) = c_\mathrm{b} + \frac{i_+ x}{D_+ F v_- (z_+ - z_-)} \tag{6}$$

Here x is defined as zero at the channel entrance and L at the etch front. $v_\pm$ is the number of positive and negative ions per salt molecule. We then calculate the limiting current density using eqn (6).

$$i_\mathrm{lim} = \frac{c_\mathrm{max}}{L} D_+ F v_- (z_+ - z_-) \tag{7}$$

Here c_max [mol m^{-3}] is the maximum solubility of chromium in the etchant. Eqn (7) states that the limiting current density is determined by the maximum solubility of chromium and the length of the channel. As a consequence the same limitation holds for the maximum obtainable etch rate.

By substituting eqn (5) and (6) into (3a) and substituting the result in (4) we are able to solve eqn (4). The result is given in eqn (8) and with this equation we can compare our theory with experimental data.

$$L = \sqrt{2\frac{MW}{\rho}\left(1 - \frac{z_+}{z_-}\right) D_+ c(L)\, t} \tag{8}$$

As mentioned above the concentration at the etch front depends on the potential difference between the metal and the electrolyte. With eqn (8) the influence of changes in the concentration of chromium at the etch front on the etch rate can be clearly seen. The influence of migration can be assessed using the $(1 - z_+/z_-)$ term in eqn (8). Furthermore, it shows that the etch rate is not a function of the lateral dimensions of the channel. This corresponds with the experimental observations made in ref. 14.

Eqn (7) shows that the current and thus the etch rate is limited by the maximum solubility of chromium in the etchant. However, as mentioned above $c(L)$ counteracts electric potential difference and, therefore, in galvanically coupled sacrificial layers, $c(L)$ does not necessarily have to be equal to the maximum solubility of the metal in the etchant. The actual kinetics of this process as a function of the potential difference between the metal couple and the etchant can be examined by performing polarization measurements.[17] Such experiments usually consist of three steps. First, the potential where there is zero current (the anodic and cathodic currents are equal to the corrosion current, i_corr) is determined. This is the potential at which etching occurs naturally and we will further refer to this potential as the corrosion potential, E_corr. The magnitude of E_corr is determined by the choice of metals and etchant. Second, the potential is scanned through values lower than E_corr. In this potential regime reduction at the cathode (*i.e.* reduction of the etchant) will be the dominant reaction. Third, the potential is scanned through values higher than E_corr. At these potentials oxidation at the anode (*i.e.* oxidation/etching of chromium) will be the dominant reaction. Because we are interested in the kinetics of the etching reaction only the first and third step are performed. If during this experiment the electric current between the couple and the electrolyte is monitored, a polarization plot can be obtained. In order to compare the results of these measurements with theory we use the current–voltage characteristic from ref. 17.

$$i = \frac{-\exp\left[z_+ F\left(E - E_\mathrm{corr}\right)/RT\right]}{\frac{1}{i_\mathrm{corr}} + \frac{1}{i_\mathrm{lim}}\exp\left[z_+ F\left(E - E_\mathrm{corr}\right)/RT\right]} \qquad c(L) >> c_\mathrm{b} \tag{9}$$

This equation is only valid for our system if $c(L) \gg c_b$. This equation describes the oxidation/etch current as a function of the potential between the metal and the electrolyte, E, and takes both the reaction kinetics and the current limitation by mass transport into account. We will present the results of these measurements below.

3 Experimental

3.1 Fabrication

We have fabricated 4 mm long, 5 μm wide and 50 nm high nanochannels with 1000 integrated electrodes. The electrodes are 3 μm wide and 1 μm separated and run across the entire channel width. In our system the metal couple is chromium and gold, where only the chromium acts as the sacrificial part. The gold remains, because it is inert to the etchant, and forms the integrated electrodes. As an etchant standard chromium etch (Merck, 111547.2500) is used. The active component (*i.e.* oxidizing species) in this etchant is cerium(IV). The fabrication process is described in Fig. 3.

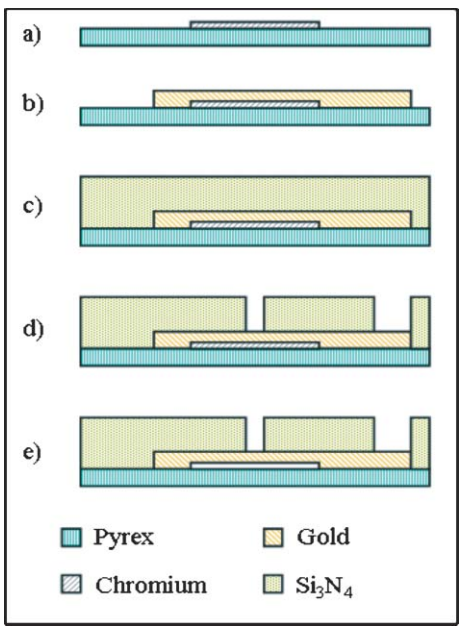

Fig. 3 Fabrication process: (a) deposition of a sacrificial chromium layer, (b) deposition of gold electrodes, (c) deposition of a 2 μm nitride layer by PECVD, (d) ion beam etching of access holes, and (e) standard wet chemical etching of the sacrificial chromium layer.

3.2 Methods

We attached the chip to the bottom of a Petri dish and made all necessary electric connections (see Fig. 4). Subsequently, we added etchant such that the chip and the additional electrodes, necessary for the experiments, were immersed. We observed the etching process using an inverted microscope (Leica DM IRM) equipped with a digital camera (Olympus CC-12) focused at the etch front. During etching we also measured the potential between the chromium/gold couple and the etch solution using a potentiostat (PARSTAT 2263) and a double junction AgAgCl/saturated KCl/saturated KNO_3 reference electrode

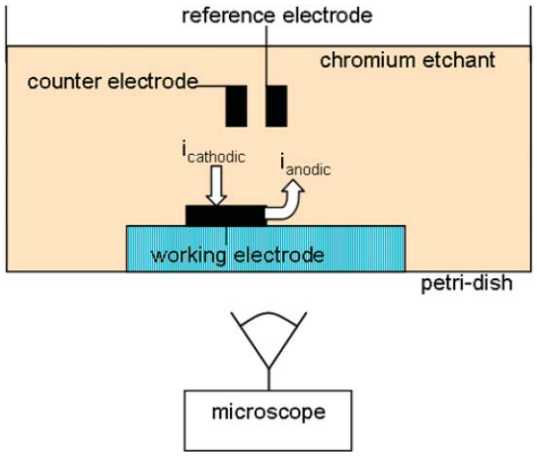

Fig. 4 Schematical representation of the experimental setup. The device is connected with its chromium/gold couple to the working electrode of the potentiostat by conductive paint and subsequent silicone coating for isolation.

(Radiometer REF251). The reason we used a double junction reference electrode is to prevent the introduction of chloride ions to the system which may influence the etch process. In Fig. 4 a schematic of the experimental setup is given. As mentioned above the reaction occurs at E_{corr}, which can be measured by applying a potential to the system such that there is no net current (*i.e.* the cathodic and anodic currents cancel) between the chromium/gold couple and the electrolyte. Furthermore, we performed potential sweeps 300 mV beyond E_{corr}, and meanwhile we observed the movement of the etch front with the microscope.

4 Results and discussion

Fig. 5 shows a channel which has been partially etched. In this micrograph the etch front can be clearly observed.

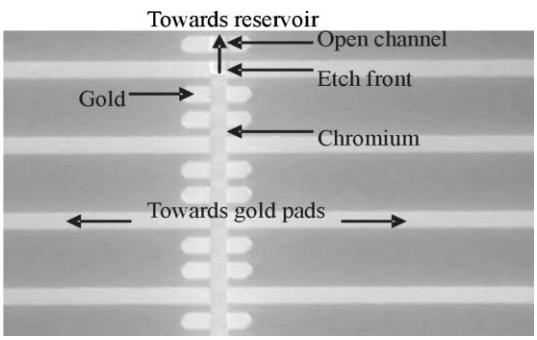

Fig. 5 Micrograph of the device during etching at 63× magnification.

During etching we monitored the movement of the etch front as a function of time. The results of this measurement are given in Fig. 6.

To determine the theoretical etch behavior we compared the experimental data to eqn (8), while using $c(L)$ as a fit parameter. The results are given in Fig. 6. Clearly, the theoretical fit and the measurements coincide well. However, for smaller etch distances the etch rate appears to be slower. This could indicate that first a chromium oxide layer needs to be removed.

Comparison of the presented value of $c(L)$ to the maximum solubility of chromium in the etchant (*i.e.* 5.5 M) shows that the

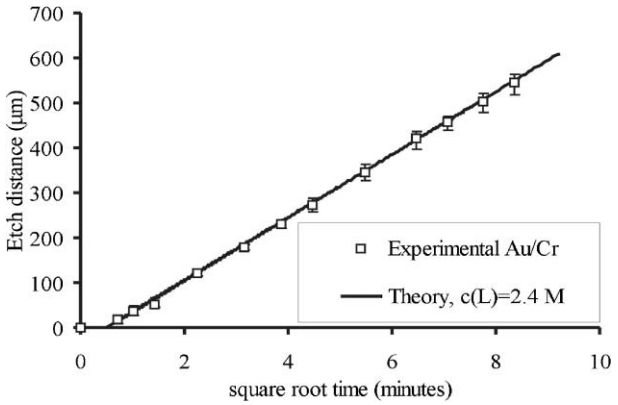

Fig. 6 Position of the etch front with respect to the channel entrance as a function of the square root of time. The error bars represent the variation in data of 5 different experiments.

etch rate is not at its theoretical maximum. Therefore, increasing the potential of the metal couple with respect to the etchant should theoretically increase the etch rate. To investigate the influence of a change in potential on the etch rate, we performed polarization measurements, as described above. We observed clear changes in the etch rate upon the application of different potentials. The measurements were performed after 700 μm of the channel had been etched. In Fig. 7 we plotted the current density as a function of an externally applied potential. The experimental curve is obtained by optical inspection of the etch front. The current density is calculated by dividing the measured currents by the cross-sectional area of the channel. Moreover, we plotted two theoretical curves based on eqn (9). Fig. 7 shows that by increasing the potential beyond E_{corr} the anodic current density (*i.e.* the etch rate) increases, and by decreasing the potential it decreases. We observed that by applying an external potential to the metal couple the etch rate can be further increased by a factor of two in comparison to a galvanic couple without an externally applied potential. Furthermore, the figure shows that there is a maximum current density, i_{lim}, determined by the maximum concentration of chromium at the etch front as predicted in the theoretical section. Fig. 7 shows that at i_{lim} the theoretical curves are in good agreement with the experiments. However, using the tabulated value of the solubility of chromium the current density is slightly overestimated. This is probably caused by the fact that we did not take the conductivity of the etchant into account which results in an overestimation of the current density for a given concentration difference. The reason for this is that the potential difference in the system also causes a migration current of the ions in the etchant and, therefore, a part of the migration current is carried by these ions and not by the chromium ions.

In Fig. 7 we also plotted a Tafel slope which describes the current density as a function of potential if the chromium dissolution is primarily determined by the reaction kinetics and mass transport does not play a role.[17] Fig. 7 shows that at current densities below i_{lim} the experimental curve does neither coincide well with the theoretical curve, nor with the theoretical Tafel slope. This indicates that the etch rate at this etch distance (700 μm) is determined by mass transport rather than reaction kinetics.

To further test our characterization we compared our results with experimental data of a copper/chromium sacrificial layer presented in ref. 14. The results of the comparison are given in Table 1 and show that our theoretical analysis is in close agreement with values given in the literature.

Finally, we consider some consequences of our theory for the design of future nanochannel devices. For devices longer than 4 mm the measured etch rates will still be somewhat slow, so in order to further increase the etch rate, E_{corr} should be increased.

Table 1 Experimental and theoretical etch rates. Literature and present values

	Present data [μm/sqrt(min)]	Literature data[14] [μm/sqrt(min)]
Experimental	65	72
Theoretical	64.8	74.7

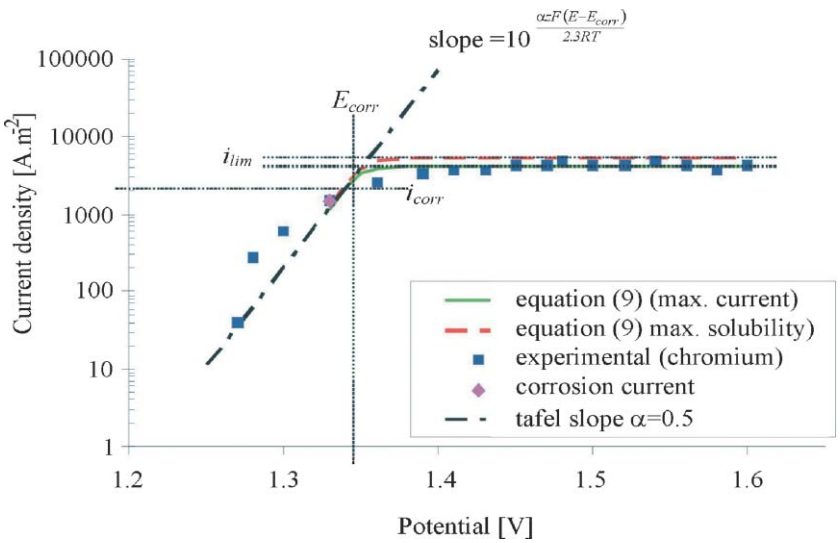

Fig. 7 Polarization measurements including theoretical curves. The theoretical curves are determined using eqn (9) in two ways. Green line: *via* the maximum measured current; red dashes: *via* the tabulated value of the maximum solubility.

Table 2 Predicted etch properties for a 1 mm long nanochannel

Material	Counter ion	c_{max} [M]	i_{lim} [A/m^2]	Maximum etch rate [μm/sqrt(min)]	Etch time [min]
Chromium	Nitrate	5.5	5413	107	22
Copper	Nitrate	5.0	4107	95	28
Aluminium	Chloride	3.2	3961	91	30

This can be done by applying an external potential to the metal couple as we showed above or by electrochemically increasing the potential difference between the two metals in the etchant. The potential between the two metals depends both on the choice of metals and the choice of etchant as discussed in the Theoretical section. However, as shown in Fig. 7 the maximum solubility of the metal in the etchant always determines the limiting etch rate. Therefore, in Table 2 we present the maximum obtainable etch rates for several metals, often used in micromachining. The etch rates are based on the maximum solubility in a given etchant. In our analysis we assume a channel length of 1 mm.

Table 2 shows that for chromium and aluminium the highest and lowest etch rates can be obtained, respectively, which is a useful observation if an external potential is applied. Differences, however, are small. If to reduce the complexity of etch setup no external potential is applied, Table 2 can be used as a guideline, however, the inherent properties of the metals and the etchant should also be considered. For example, if we consider chromium as the sacrificial metal, it should be noted that chromium appears to have a higher standard electrode potential than expected from the literature,[14] which effectively decreases its potential with respect to that of the etchant and of the more cathodic metals. This is according to ref. 19 caused by its passivity effect which is an energy barrier on the chromium/electrolyte interface. The same holds for aluminium, which appears to have the advantage that it is very low in the electrochemical series, which means that the potential difference with almost any other metal (which is suitable for micromachining) will be high. Therefore, in order to decide on the metal couple with the highest etch rate additional experiments with different metals are necessary.

5 Conclusions

We present an etch method for surface micromachining of nanochannels with bare integrated electrodes using a single metal sacrificial layer. An advantage of the etch method is that it is ten times faster than conventional sacrificial methods. Furthermore, a theory based on mass transport using the Nernst–Planck equations is presented that describes the observed etch rates well. To further investigate the kinetics of the etch process we performed polarization measurements. These measurements indicate that etch rates can be further increased by a factor of two by applying an external potential to the metals. The theory we developed enables predictions of etching behavior for future devices using externally applied potentials. For systems employing different sacrificial or electrode metals, however, additional experiments are necessary.

Acknowledgements

Nanoned is gratefully acknowledged for the financial support of this project *via* a Nanoned grant.

References

1 J. Eijkel and A. Van Den Berg, *Microfluidics Nanofluidics*, 2005, **1**, 249–267.
2 D. Mijatovic, J. Eijkel and A. Van Den Berg, *Lab Chip*, 2005, **5**, 492–500.
3 J. Haneveld, H. Jansen, E. Berenschot, N. Tas and M. Elwenspoek, *J. Micromech. Microeng.*, 2003, **13**, S62–S66.
4 R. Karnik, R. Fan, M. Yue, D. Li, P. Yang and A. Majumdar, *Nano Lett.*, 2005, **5**, 943–948.
5 A. Plecis, R. B. Schoch and P. Renaud, *Nano Lett.*, 2005, **5**, 1147–1155.
6 M. B. Stern, M. W. Geis and J. E. Curtin, *J. Vac. Sci. Technol. B*, 1997, **15**, 2887–2891.
7 A. Han, N. F. de Rooij and U. Staufer, *Nanotechnology*, 2006, **17**, 2498–2503.
8 J. C. T. Eijkel, J. Bomer, N. R. Tas and A. Van Den Berg, *Lab Chip*, 2004, **4**, 161–163.
9 M. Foquet, J. Korlach, W. Zipfel, W. W. Webb and H. G. Craighead, *Anal. Chem.*, 2002, **74**, 1415–1422.
10 S. W. Turner, A. M. Perez, A. Lopez and H. G. Craighead, *J. Vac. Sci. Technol. B*, 1998, **16**, 3835–3840.
11 N. R. Tas, J. W. Berenschot, P. Mela, H. V. Jansen, M. Elwenspoek and A. Van Den Berg, *Nano Lett.*, 2002, **2**, 1031–1032.
12 W. L. Li, J. O. Tegenfeldt, L. Chen, R. H. Austin, S. Y. Chou, P. A. Kohl, J. Krotine and J. C. Sturm, *Nanotechnology*, 2003, **14**, 578–583.
13 D. A. Czaplewski, J. Kameoka, R. Mathers, G. W. Coates and H. G. Craighead, *Appl. Phys. Lett.*, 2003, **83**, 4836–4838.
14 H. Zeng, Z. Wan and A. D. Feinerman, *Nanotechnology*, 2006, **17**, 3183–3188.
15 G. Fuhr, R. Hagedorn, T. Müller, W. Benecke and B. Wagner, *J. Microelectromech. Syst.*, 1992, **1**, 142–146.
16 A. Ramos, H. Morgan, N. G. Green, A. González and A. Castellanos, *J. Appl. Phys.*, 2005, **97**, Art. No. 084906.
17 A. J. Bard and L. R. Faulkner, *Electrochemical methods: Fundamentals and applications*, Wiley Interscience, 2nd edn, 2001, ISBN 978-0-471-04372-0.
18 R. F. Probstein, *Physicochemical hydrodynamics: An introduction*, Wiley Interscience, 2nd edn, 1994, ISBN 0-471-45830-9.
19 H. P. Hack, *Galvanic corrosion*, ASTM, Philadelphia, PA, 1988.